Contents lists available at ScienceDirect

Arabian Journal of Chemistry

journal homepage: www.ksu.edu.sa

Original article

Enhanced flame retardancy and thermal stability in flexible polyurethane foam through synergistic core-shell structured DBDPE@PMA particles

Xuping Ni [a], Lingjie Wu [b,c,*]

[a] College of Intelligent Architecture, Zhejiang College of Security Technology, Wenzhou 325016, China
[b] College of Civil Engineering and Architecture, Wenzhou University, Wenzhou 325035, China
[c] Key Laboratory of Engineering and Technology for Soft Soil Foundation and Tideland Reclamation of Zhejiang Province, Wenzhou 325035, China

ARTICLE INFO

Keywords:
Core-shell particles
Flame retardancy
Decabromodiphenyl ethane
Flexible polyurethane foam

ABSTRACT

This research presents the synthesis of core–shell structured flame retardant particles, DBDPE@PMA, which combines the flame-retardant and toughening functions. These particles utilize decabromodiphenyl ethane (DBDPE) as the core and a copolymer of methyl methacrylate and acrylic acid (MMA-AA) as the shell, which are created via emulsion polymerization. The process involved an initial reaction of DBDPE@PMA with isocyanate, followed by foaming with polyether polyol to fabricate flame retardant, and the flexible polyurethane foam (P/D-FPUF) was thermally insulated. The study examined the influence of DBDPE@PMA on the flame retardancy properties of flexible polyurethane foam. Scanning electron microscopy confirmed the encapsulation of DBDPE by the polymer, resulting in a core–shell composite particle. The interaction between the carboxylic groups (–COOH) on the DBDPE@PMA shell and isocyanate enhanced the interfacial bonding, thereby increasing the foam's apparent density and ensuring better integration with the polyurethane matrix. However, DBDPE@PMA had aggregates on the foam matrix bubble holes, resulting in uneven bubble holes. DBDPE@PMA markedly improved the flame retardancy and thermal stability of the foam, compared to both pure polyurethane and foam containing solely DBDPE (10D-FPUF). The oxygen index value of the foam with 20% DBDPE@PMA (20P/D-FPUF) reached 33.6%, with UL-94 horizontal and Vertical burning level tests achieving the highest classifications. The char residue after thermal degradation increased significantly from 1.93% in pure foam to 5.06%. While the smoke density level rose, the duration to peak smoke density was prolonged to 78 s, offering an enhanced margin for evacuation during the initial stages of a fire.

1. Introduction

Flexible polyurethane foam (FPUF) is extensively utilized across various industries, including furniture, construction, and automotive, owing to its outstanding properties such as light weight, softness, sound absorption, and thermal insulation (Zhang et al., 2022). Despite these advantages, FPUF's limited thermal stability, low ignition threshold, rapid combustion, intense flame propagation, the generation of toxic fumes and molten droplets during burning pose significant challenges to its applications (Zhu et al., 2022).

To mitigate these fire hazards, researchers have explored numerous flame-retardant strategies, primarily incorporating flame retardants during synthesis or altering the molecular structure of FPUF components (Li et al., 2024). Common flame retardants for FPUF include: (1) Halogenated retardants, which function in the gas phase to quench free radicals and disrupt combustion chain reactions, thereby reducing combustible gas concentrations and oxygen availability (Lee et al., 2022); (2) Phosphorus-based retardants, which promote char formation in the condensed phase, creating a barrier against air and heat transfer while diminishing the release of flammable gases (Rao et al., 2018a; Zhou et al., 2020; Qin et al., 2021); (3) Nitrogen-based retardants, which inhibit heat exchange by decomposing into non-flammable gases that absorb heat and lower temperatures (Li et al., 2023b; Meng et al., 2023); (4) Inorganic retardants, which absorb significant heat upon decomposition, contributing to flame retardancy (Nabipour et al., 2020; Weldemhret et al., 2021).; and (5) Intumescent retardants, such as expandable graphite, melamine, and ammonium polyphosphate, which swell when heated, forming a protective char layer that resists high temperatures and oxygen (Chan et al., 2021; Chan et al., 2022; Li et al., 2023a; Wang et al., 2023).

* Corresponding author at: College of Civil Engineering and Architecture, Wenzhou University, Wenzhou 325035, China.
E-mail address: wulingjie01@wzu.edu.cn (L. Wu).

https://doi.org/10.1016/j.arabjc.2024.105684
Received 10 January 2024; Accepted 10 February 2024
Available online 12 February 2024

Despite their effectiveness, these flame retardants have some drawbacks. Nitrogen-based flame retardants are often associated with higher costs, reduced durability, and less efficient flame retardation. Phosphorus-based retardants may migrate or volatilize, lack durability, and are costly. Inorganic and intumescent retardants often require large quantities, potentially compromising mechanical properties and exhibiting poor interfacial compatibility with the FPUF matrix (Lee et al., 2022). Structural modification, while preserving mechanical integrity and offering persistent flame retardancy, is complex and expensive. Additionally, the performance of many flame retardants can diminish over time due to environmental factors. Consequently, brominated flame retardants, especially for decabromodiphenyl ethane (DBDPE), remain a preferred choice due to their high bromine content (82.3 %), excellent light and UV stability, thermal resilience, and recyclability (Rao et al., 2018b).

Nonetheless, incorporating flame retardants can inadvertently increase the thermal conductivity of FPUF, reducing its insulative capacity. To address these limitations, novel core–shell structured flame retardants have been proposed. These include carbon black nanoparticles with a core–shell structure (CB@KF) synthesized via in situ polymerization (Xia et al., 2022), mechanically fused composite particles for synergistic flame-retardant studies (Kim et al., 2023). In addition, a new intumescent gel silicon/polyammonium phosphate core–shell retardant (MCAPP) was also included for examining PU composites' flame resistance, thermal stability, and water resistance (Ni et al., 2011). Hierarchical core–shell structured frameworks, such as CMSs@LDH@PZN, have been developed to enhance polypropylene's flame retardancy (Zhong et al., 2022). Additionally, covalently bonded SiO2@UiO-66 (Guo et al., 2019; Wang et al., 2021), and chitosan@MMT encapsulated ammonium polyphosphate (APP@CS@MMT) core–shell flame retardants have been incorporated into TPU matrices to improve flame retardancy and smoke suppression (Shi et al., 2024). Moreover, aluminum hydroxide-coated expanding graphite (EG@ATH) has been used to bolster the flame resistance of rigid polyurethane foam (RPUF) (Wang et al., 2017). Acrylic/methyl methacrylate copolymers, with their excellent elasticity and functional groups, have been widely employed as the shell material in core–shell particles due to their ease of preparation and structural control (Li et al., 2008; Zhang et al., 2011). Despite advancements in the fundamental and applied research of core–shell structured polymers, further investigation into the structural design, synthesis of composite particles, and their impact on FPUF's flame retardancy is imperative.

In this study, we introduce a structural design that employs DBDPE as the core and a reactive MMA-AA copolymer as the shell. We synthesize DBDPE@PMA core–shell particles with dual flame-retardant and toughening functions through emulsion polymerization. These particles are chemically bonded to the FPUF matrix, enhancing the interfacial interaction and overall flame retardancy. This approach also aims to preserve thermal insulation and reduce fire hazards, providing a theoretical framework and practical insights for the application of insulating polyurethane materials in construction and industrial settings.

2. Experimental procedure

2.1. Raw materials

The raw materials required for the experiments, along with their material performance parameters, are as follows: polyether polyol with a molecular weight of 3000 to 5000; dibutyltin dilaurate (Dabco T-9), with a relative molecular mass of 405.1, containing more than 96 % tin, which is a product of Air Products and Chemicals, Inc., USA; Industrial grade silicone oil as a foam stabilizer; triethylenediamine (A33) used as a strong gel catalyst; laboratory-made deionized water used as a blowing agent; toluene diisocyanate (TDI) used in an 80/20 ratio; DBDPE, conforming to QB/YT01-2005 standard, supplied by Jinan Jinyingtai Chemical Co., Ltd.; methyl methacrylate (MMA) and acrylic acid (AA) both of analytical grade, from Chengdu Kelong Chemical Reagent Factory; and ammonium persulfate (APS) and sodium dodecylbenzenesulfonate (SDBS) also of analytical grade, likewise produced by Chengdu Kelong Chemical Reagent Factory.

2.2. Experimental preparation

2.2.1. Preparation of Core-Shell flame retardant particles

To prepare the core–shell flame retardant particles, we began by dissolving 1.2 g of the emulsifier SDBS in 100 ml of deionized water at 50 °C to achieve full emulsification, facilitated by a magnetic stirrer in a constant temperature water bath. Following this, 0.5 g of APS was added as an initiator. Once fully dissolved, a 1:1 mixture of MMA and AA totaling 100 ml was introduced dropwise using a constant pressure dropping funnel, and the reaction was continuously stirred for 5 h. The resultant PMA emulsion was cooled to room temperature, filtered through a Büchner funnel lined with filter paper under reduced pressure, and then dried in a vacuum oven at 60 °C to yield PMA particles post-grinding.

For the core–shell particles, the procedure mirrored that of the PMA particles, as shown in Fig. 1, with the addition of 100 g of DBDPE to the initial emulsification process. The resulting material, after polymerization, filtration, and drying, was the core–shell structured flame retardant particles DBDPE@PMA, with DBDPE as the core and PMA as the shell.

2.2.2. Preparation of flame retardant flexible polyurethane foam

Following the recipe outlined in Table 1, we measured specific amounts of polyether polyol, TDI, A33, T-9, silicone oil, water, and the flame retardant core–shell particles DBDPE@PMA or DBDPE alone. Initially, DBDPE@PMA or DBDPE were blended with TDI at high speed. This mixture was then combined with a second mixture containing polyether polyol, silicone oil, water, A33, T-9, and other additives. After stirring for 4–10 s at high speed, the mixture, upon turning white, was promptly poured into a mold. The resulting foam was cured at room temperature (23 °C) for 24 h before demolding to produce the novel flame retardant and thermally insulating flexible polyurethane foam (P/D-FPUF). The process flow is depicted in Fig. 2.

2.3. Testing and characterization

2.3.1. Structural characterization

A JSM-7001F field emission scanning electron microscope (SEM) was employed to observe the microstructure and morphology of DBDPE, PMA, DBDPE@PMA, and FPUF. The SEM's resolution was set to 1.2 nm at 30 kV and 3.0 nm at both 1 kV and 15 kV (WD10 mm, 5nA), with an acceleration voltage range of 0.2 kV to 30 kV and magnification capabilities from × 10 to × 1000000. The influence of core–shell particles on the FPUF morphology was analyzed.

2.3.2. Apparent density

The apparent density of the polyurethane foam samples was determined after a 72-hour conditioning period at 25 °C and 50 % relative humidity. The samples were processed to dimensions of 200 mm × 100 mm × 30 mm, and their volume and mass were measured using a vernier caliper and an electronic balance, respectively. The apparent density was calculated, with an accuracy of 0.1 kg/m^3, and the average value from five samples was recorded.

2.3.3. Oxygen index test

The limiting oxygen index (LOI) values were ascertained using an HC-2 type oxygen index meter, according to the GB/T2406-1993 standard. The top ignition method was used, and the sample dimensions were 130 mm × 10 mm × 10 mm.

2.3.4. UL-94 horizontal and vertical burning test

A CZF-3 type horizontal and vertical burning tester were employed in

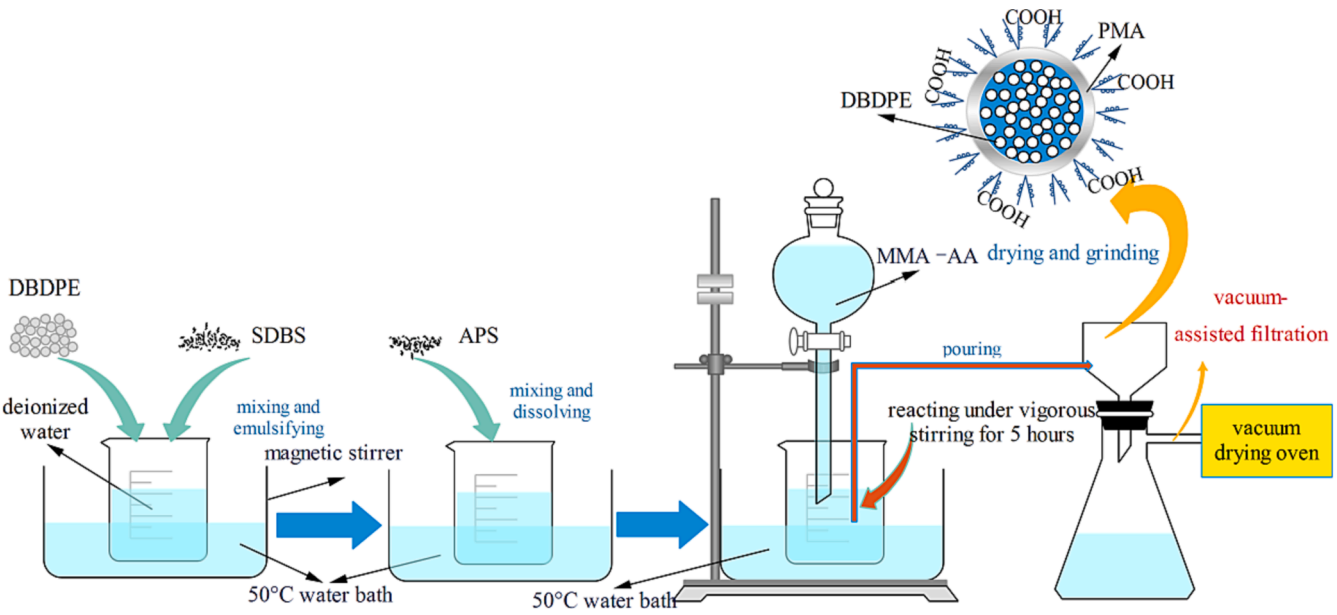

Fig. 1. Schematic for synthetic route of DBDPE@PMA.

Table 1
Composition of Raw Materials for P/D-FPUF.

Sample	Polyether polyol /g	TDI /g	silicone oil /g	Water /g	A33 /g	T-9 /g	DBDPE	Core-shell particles /g
FPUF	100	40	7	1.5	0.8	0.9	0	0
5P/D-FPUF	100	40	7	1.5	0.8	0.9	0	5
10P/D-FPUF	100	40	7	1.5	0.8	0.9	0	10
15P/D-FPUF	100	40	7	1.5	0.8	0.9	0	15
20P/D-FPUF	100	40	7	1.5	0.8	0.9	0	20
10D-FPUF	100	40	7	1.5	0.8	0.9	10	0

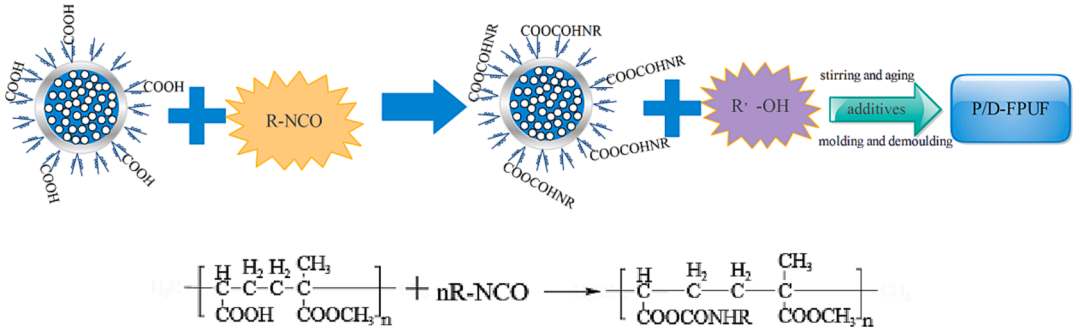

Fig. 2. Preparation of P/D-FPUF.

accordance with GB/T4609-1996 to assess the burning grade. The flame time, non-flame time, dripping, and other combustion phenomena were recorded for samples measuring 130 mm × 13 mm × 13 mm.

2.3.5. Smoke density test

Conforming to GB/T 8627–2007, a YM-3 type tester for measuring smoke density of building material was utilized to evaluate the smoke density of the samples, which were sized at 25.4 mm × 25.4 mm × 10 mm. The corresponding observations included the melting, dripping, foaming, and charring.

2.3.6. Thermogravimetric test

The thermal stability of FPUF, 10P/D-FPUF, and 10D-FPUF samples was measured using a NETZSCH TG 209F1 Iris thermogravimetric analyzer. The analysis was performed under a nitrogen atmosphere, with a heating rate of 10 °C/min and a temperature range extending from room temperature to 600 °C.

3. Results and discussion

3.1. Characterization of flame retardants

The SEM images presented in Fig. 3 reveal the morphological characteristics of DBDPE, PMA, and DBDPE@PMA particles. The DBDPE particles exhibit a broad size distribution, ranging from 1 to 4 μm, and assume an irregular, near-spherical shape with a propensity to agglomerate into clusters. This agglomeration and the uneven dispersion observed may stem from incomplete reactions during synthesis, limitations in separation, purification techniques, and environmental conditions (e.g., temperature and humidity).

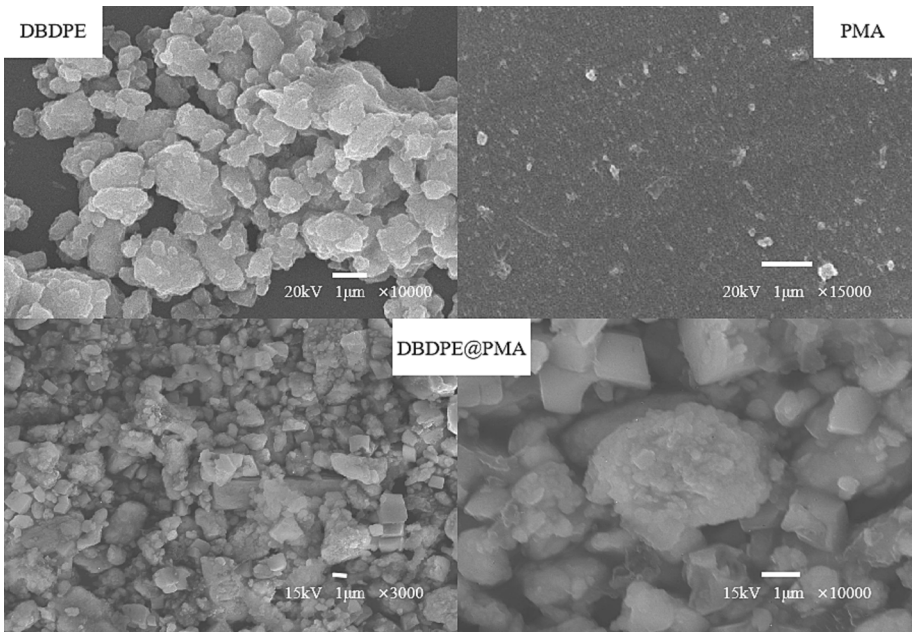

Fig. 3. SEM images of DBDPE, PMA, and DBDPE@PMA.

In contrast, PMA particles are markedly smaller, with dimensions spanning from 0.05 μm to 0.5 μm, and are characterized by a smooth surface. Despite their size uniformity, they demonstrate small gaps and interfaces between particles, potentially attributable to incomplete compaction or surface roughness (Zhang et al., 2011; Zhu et al., 2022).

From the SEM images of the core–shell particles DBDPE@PMA at different magnifications, it can be observed that, compared to DBDPE, the surface morphology of the core–shell particles would become rougher. In addition, the particle size has increased, and the dispersion is more uniform. Although, there are defects in the polymer coating the particles, such a phenomenon demonstrates the successful microencapsulation of PMA on DBDPE (Zhang et al., 2011). This is because during the drying and dehydrating process, particle evaporation can leave behind defects, leading to particle agglomeration with the formation of aggregates. The diameter of these aggregated particles can reach up to 5 μm. Direct incorporation into the preparation of polyurethane foam may affect the dispersion and pore size of the foam cells (Han et al., 2023; Wang et al., 2023).

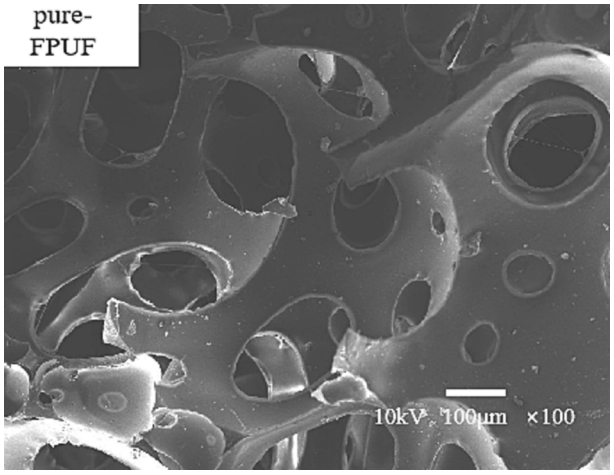

Fig. 4. SEM image of pure FPUF.

3.2. Apparent density and foam morphology analysis

Fig. 4 shows the SEM images of pure FPUF, which reveals an intact structure with uniformly open pores and a consistent pore size, resulting from the gas generation and nucleation processes during foaming. The resultant network-like structure solidifies into a porous foam plastic.

The comparative SEM analysis of 10P/D-FPUF and 10D-FPUF, as indicated in Fig. 5, demonstrates that 10P/D-FPUF maintains a uniform cell morphology with a fuzzy interface between the DBDPE@PMA particles and FPUF matrix, indicative of close binding and compatibility. Compared to the pure FPUF samples, there is an emergence of uneven cell sizes, with the largest pores reaching up to 600 μm, and a greater number of open cells. The foam still consists of a large number of cell struts, and the core–shell particles are distributed relatively evenly on the struts of foam matrix, though there are some agglomerates formed. The core–shell particles on the foam struts are mostly polygonal in shape, with smooth surfaces, retaining their morphology well. This is mainly because the –COOH on DBDPE@PMA can chemically react with the –NCO of TDI to form -COOCOHNR groups, enhancing the interfacial interaction and compatibility, allowing it to enter the FPUF matrix effectively (Zhang et al., 2011). However, because the particles are fine and have high surface energy, they tend to agglomerate. This makes it difficult to disperse them evenly in FPUF, leading to uneven distribution of the core–shell particles.

The foam structure of 10D-FPUF is more intact, composed of a large number of cell struts forming a strut network, but the cells are relaxed and irregular. The distribution of DBDPE particles on the foam structure is more uneven, with poor compatibility, resulting in uneven cell sizes. The gaps between DBDPE and FPUF are larger than those between DBDPE@PMA particles and FPUF, with the largest pores reaching up to 1 mm. Therefore, when the matrix is subjected to external forces, stress cannot be effectively transferred from the matrix to DBDPE particles, leading to the reduction of the mechanical properties. However, because DBDPE@PMA is chemically bonded to the matrix, stress can be transferred from the matrix to DBDPE particles, thus improving mechanical properties (Ye et al., 2009; Karteri and Ozyesildag, 2021). Additionally, in the magnified SEM images, DBDPE particles appear irregular in shape with rough surfaces and presence of agglomerates, indicating that the addition of DBDPE affects the nucleation of the foam cells and has poor compatibility with the foam.

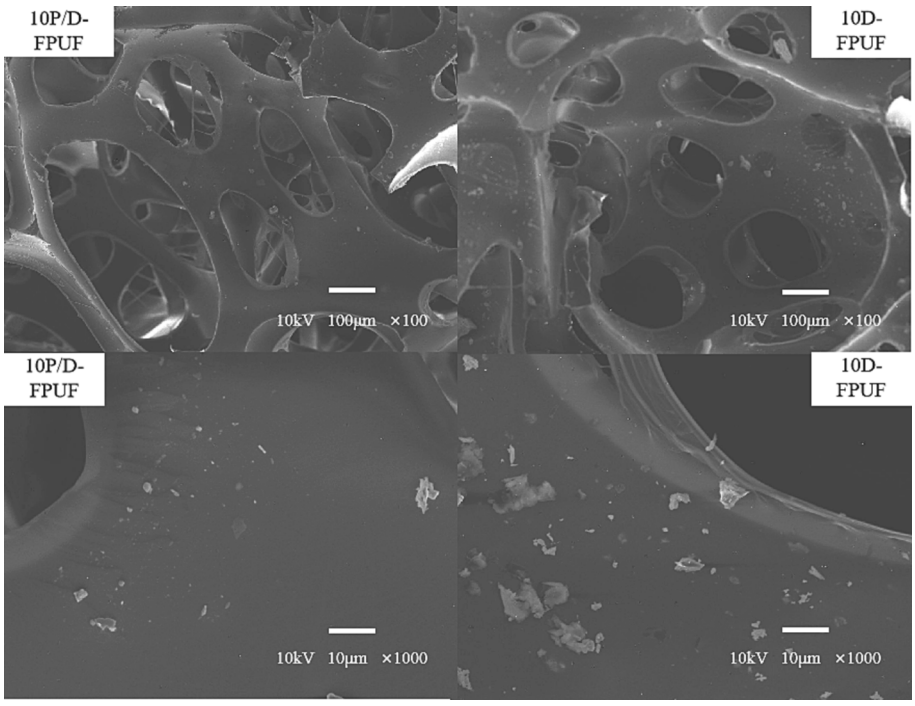

Fig. 5. Cross-sectional SEM images of 10P/D-FPUF and 10D-FPUF.

The relationship between the addition of various flame retardants and apparent density of flexible polyurethane foam is depicted in Fig. 6. The density of the pure FPUF is noted to be 1036.9 kg/m^3. The addition of flame retardants results in an increase in the density of the polyurethane foam, with densities for 5P/D-FPUF, 10P/D-FPUF, 15P/D-FPUF, 20P/D-FPUF, and 10D-FPUF recorded at 1422.1 kg/m^3, 1497.1 kg/m^3, 1582.4 kg/m^3, 1600.9 kg/m^3, and 1502.4 kg/m^3, respectively. This indicates that after adding flame retardants, they act as nucleating agents during the foaming process of FPUF, leading to the formation of more foam cells. This affects the cellular structure of the polyurethane material, resulting in smaller cell diameters and, consequently, an increased density of the flame-retardant polyurethane foam. However, the presence of agglomerates results from the added flame retardants, which can disperse unevenly and leads to non-uniform cell sizes. When the same mass of DBDPE and DBDPE@PMA is added, the density of 10P/D-FPUF is lower. This is because DBDPE@PMA is chemically bonded to TDI, which has a smaller impact on the foaming reaction, while DBDPE is physically dispersed within the matrix. DBDPE interacts weakly with the RPUF base due to the lack of chemical reaction, leading to uneven dispersion and significant agglomeration. Thus, the foam matrix would be negatively impacted (Ni and Wu, 2023).

3.3. Flame retardancy studies

The flame retardancy of the materials in this study was evaluated using the LOI tests, UL-94 horizontal and vertical burning tests. An elevated LOI value signifies a greater oxygen requirement for combustion, implying enhanced flame resistance. Materials with an LOI below 21 % are deemed flammable, those with an LOI between 21 % and 27 % are considered combustible. Meanwhile, those exceeding 28 % are classified as flame-retardant. The UL-94 tests provide a qualitative measure of flame retardancy by observing burning behavior, combustion duration, and rate in both horizontal and vertical orientations to

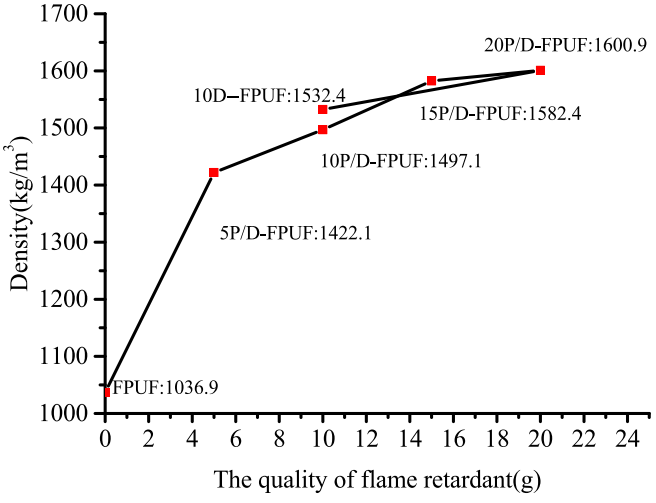

Fig. 6. Apparent densities of FPUF, P/D-FPUF, and 10D-FPUF.

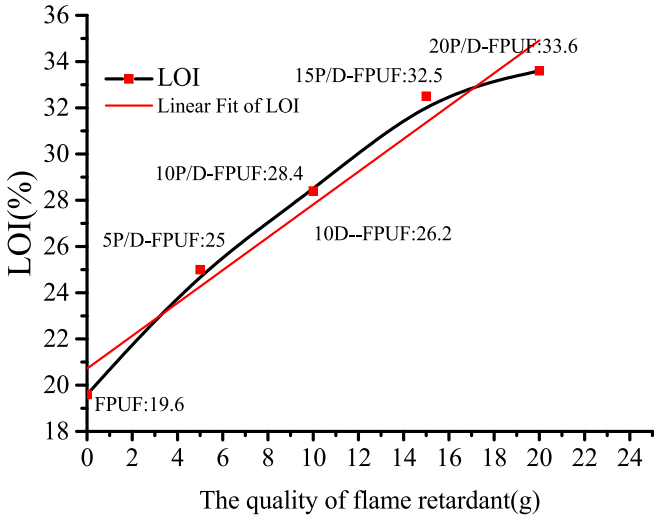

Fig. 7. Results of the LOI value of Flame-retardant flexible polyurethane foam.

assign a burn rating (Ni and Wu, 2023).

Fig. 7 shows the LOI values for flexible polyurethane foam samples with varying concentrations of flame retardants. The LOI for the pure FPUF (Sample A) is 19.6 %, which categorizes it as combustible. It burns with dripping and emits noxious gases. An increase in the LOI is observed with the addition of core–shell flame-retardant particles, with a 20 g addition elevating the LOI to 33.6 %. Hence, the national standard and achieving flame-retardant status are surpassed. This enhancement is attributed to the reaction between the –COOH groups on DBDPE@PMA and –NCO groups of TDI, forming a stable -COOCOHNR structure that augments the thermal stability of the foam. During combustion, the DBDPE component decomposes, capturing free radicals released from the material's degradation and thereby impeding the combustion chain reaction. The evolved hydrogen bromide (HBr) acts as an inert blanket, inhibiting oxygen access to the material's surface (Lu et al., 2023).

The relationship between the LOI and addition of core–shell particles (x) is expressed as LOI $= 20.72 + 0.71x$. This linear correlation underscores the improved flame retardancy afforded by the chemically bonded flame-retardant groups within the matrix and physically incorporated flame retardants, which enhances compatibility with the FPUF.

A comparison of the oxygen index values between 10P/D-FPUF and 10D-FPUF indicates that the LOI of the foam with physically added DBDPE (10D-FPUF) is 26.2 %, which is lower than that of the core–shell particle-enhanced foam. Direct DBDPE addition results in poor compatibility with FPUF, leading to potential issues such as foam pore collapse and reduced mechanical properties due to uneven dispersion.

The outcomes of the UL-94 horizontal and vertical burning test are summarized in Table 2. In the horizontal test, the pure FPUF rapidly burned beyond the first mark line (25 mm) at a rate of 296 mm/min. Upon ignition for 30 s, the flame front edge of other samples did not reach the first mark line and self-extinguished. The incorporation of core–shell particles and DBDPE effectively reduces the horizontal burning rate of polyurethane materials and enhances their horizontal burn rating.

In vertical burning test, pure FPUF burns rapidly to the clamp, producing molten droplets that ignite the degreased cotton, which earns a classification of NR. In contrast, polyurethane samples with added core–shell flame retardant particles and DBDPE undergo vigorous combustion when ignited for 10 s. However, samples 5P/D-FPUF, 10P/D-FPUF, and 10D-FPUF produce molten droplets that also ignite the degreased cotton, yet the flames extinguish once the ignition source is removed, and they cannot be re-ignited. During the tests, it was observed that none of the samples exhibited flameless burning, and all released irritating gases. As the mass of core–shell flame retardant particles increased, there was a noticeable reduction in flaming burn time, and improvements were seen in the burning classification. Comparing 10P/D-FPUF and 10D-FPUF, it was found that the same addition level of core–shell particles and DBDPE does not significantly affect the results of the UL-94 horizontal and vertical burning tests. However, the polyurethane foam with added DBDPE exhibited more intense burning and longer burning times. This indicates that core–shell flame retardant particles have a better flame-retarding effect. That is because they are chemically bonded to TDI and have less impact on the matrix, and better compatibility would be offered. Furthermore, the increase in core–shell flame retardant particles enhances the flame-retardant effectiveness of the flexible polyurethane foam, reducing the hazard of fire (Liu et al., 2022).

Table 2
Results of UL-94 tests for Flame-retardant flexible polyurethane foam.

Sample	Burning rate mm/min	UL-94					
		t1 /s	t2 /s	Tf /s	Ignition of cotton by dripping	Presence of burning or dripping from the sample	Level
FPUF	296	20	0	105	Yes	Yes	NR
5P/D-FPUF	HB	10.2	0	51	Yes	No	FV-2
10P/D-FPUF	HB	7.6	0	38	Yes	No	FV-2
15P/D-FPUF	HB	7	0	35	No	No	V-0
20P/D-FPUF	HB	6	0	30	No	No	V-0
10D-FPUF	HB	8	0	40	Yes	No	FV-2

The LOI and burning tests conclusively show that the flame-retardant and thermally insulating FPUF with added DBDPE@PMA exhibits superior flame retardancy compared to pure FPUF and FPUF with only DBDPE added. The improved flame retardancy results from the chemical integration of DBDPE@PMA core–shell particles into the TDI, which facilitates even dispersion and minimal impact on the polyurethane reaction and compatibility. During initial decomposition, the PMA shell degrades, allowing the DBDPE core to function as a flame retardant. The bromine-based flame retardants present in both polyurethane foams operate through a gas-phase mechanism. As shown in Fig. 8, with the base foam decomposes, the flame retardants also degrade. Here, DBDPE cleaves its carbon-bromine (C-Br) bonds at elevated temperatures, and releases bromine radicals (Br·) that effectively capture the free radicals from the material's thermal degradation. This process significantly lowers the concentration of free radicals, thereby quelling or halting the combustion chain reaction. Furthermore, the evolved HBr from the decomposition of flame retardants acts as a barrier against oxygen, suppressing the combustion reaction. The core–shell particles' DBDPE@PMA also absorb heat during the shell PMA degradation, diminishing the environmental temperature and decelerating the burn rate (Wang et al., 2023; Gao et al., 2024).

3.4. Thermal stability analysis

Thermogravimetric analysis (TGA) was employed to assess the thermal performance of FPUF, 10P/D-FPUF, and 10D-FPUF materials. The TG and derivative thermogravimetry (DTG) curves for the samples are presented in Fig. 9, while Table 3 presents the details of the thermal decomposition parameters under nitrogen atmosphere, including the onset temperature of decomposition (T_{onset}), maximum decomposition temperatures (T_{1Max}, T_{2Max}), maximum rate of decomposition (V_{1Max}, V_{2Max}), the endset temperature of decomposition (T_{end}), and the char residue at 600 °C.

The thermal decomposition of all materials occurs in two distinct stages, with the initial step commencing between 200 °C and 320 °C and the subsequent step between 320 °C and 400 °C. The first stage is characterized by the scission of the soft segments within the polyurethane foam, yielding isocyanates and polyols at a relatively slow decomposition rate. The weight losses at this stage for pure FPUF, 10D-FPUF, and 10P/D-FPUF are 22.82 %, 26.43 %, and 24.38 %, respectively. The 10D-FPUF and 10P/D-FPUF samples show a slight increase in the weight loss compared to the pure FPUF, but the difference is not significant. This is attributed to the relatively high thermal stability of the added flame retardant DBDPE, which generally decomposes at temperatures ranging from 300 °C to 400 °C (Liu et al., 2016; Liu et al., 2023).

The second decomposition phase involves the breakdown of polyols and further cleavage of C-C and C-O bonds in the main chain, leading to a marked acceleration in decomposition rate and weight loss. For 10D-FPUF and 10P/D-FPUF, the T_{onset}, T_{1Max}, T_{2Max}, and T_{end} are all lower, compared to pure FPUF. This indicates that these materials undergo decomposition at reduced temperatures and may act as catalysts for the decomposition of the matrix. The relatively low bond energy of C-Br in the flame retardants leads to their decomposition within 200 °C to 300 °C, and the bond energy of C-Br bonds typically falls within the range of 275–330 kJ/mol (66–79 kcal/mol). For DBDPE, its

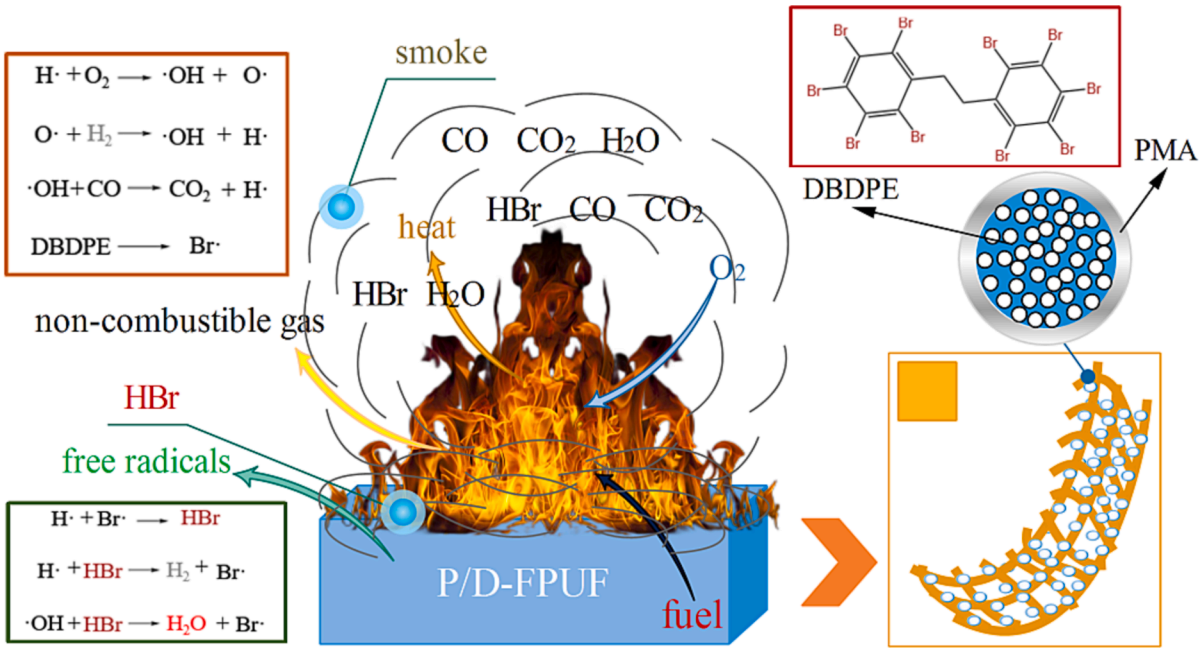

Fig. 8. Flame retardant mechanism of DBDPE.

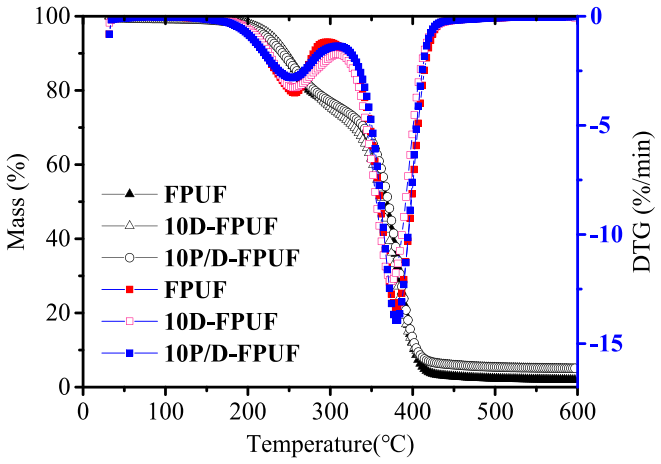

Fig. 9. TG and DTG curves of pure FPUF 10D-FPUFand 10P/D-FPUF.

decomposition temperature is between 300 °C and 400 °C, where the C-Br bonds start to cleave, releasing HBr and other bromine compounds. These released substances capture free radicals, thus inhibiting the combustion process and functioning as flame retardants (Liu et al., 2016; Liu et al., 2023). The relatively lower bond energy of C-Br within flame retardants contributes to a reduction in the decomposition rate of polyurethane foam, decreases the onset temperature for thermal degradation, and lowers the peak temperature at which the degradation rate is highest. This earlier onset of decomposition significantly enhances the effectiveness of the flame-retardant system (Eceiza et al., 2023).

At 600 °C, the char residue rates for 10D-FPUF and 10P/D-FPUF are 4.85 % and 5.06 %, respectivelyan increase that is likely due to DBDPE's intrinsic thermal stability, which enhances the overall thermal stability of the polyurethane foam to a degree. During thermal degradation, as shown in Fig. 8, Br· are generated and react with the polyurethane foam to produce HBr. HBr then reacts with the highly reactive hydroxyl radicals (OH·), regenerating Br, and diminishing the concentration of OH· radicals. Hence, suppressing the combustion chain reaction and decelerating the burn rate until extinguishment. The evolved HBr, being an inert gas, also functions to shield the material's surface, obstructing and diluting the oxygen concentration (Lu et al., 2023).

The initial degradation temperature of the PMA shell in 10P/D-FPUF is not particularly high; therefore, as DBDPE begins to decompose and release non-flammable gases, the PMA also degrades. The core–shell composite flame-retardant particles manifest their flame-retardant capabilities, and through chemical modification bonded to TDI, flame-retardant properties are imparted to the material. Consequently, the material exhibits persistent flame retardancy with minimal detriment to its mechanical properties. The flame-retardant efficacy surpasses that of polyurethane foam with a direct addition of DBDPE, significantly elevating the char residue rate and enhancing the stability of the flame-retardant system within FPUF.

3.5. *Smoke production study*

The combustion of the FPUF generates smoke, which can significantly impede firefighting efforts and evacuation, increasing the risk during a fire. Fig. 10 illustrates the smoke density variation during the combustion of P/D-FPUF with different types and amounts of flame

Table 3
Parameters of the thermal decomposition reaction of pure FPUF 10D-FPUF and 10P/D-FPUF.

Sample	T_{onset} (℃)	T_{Max} (℃)		V_{Max} (%/min)		T_{end} (℃)	Residual of mass(600℃) (%)
		T_{1Max}	T_{2Max}	V_{1Max}	V_{1Max}		
FPUF	215	257	381	3.51	13.37	407	1.93
10D-FPUF	214	256	374	3.27	12.15	402	4.85
10P/D-FPUF	207	254	380	2.81	13.97	404	5.06

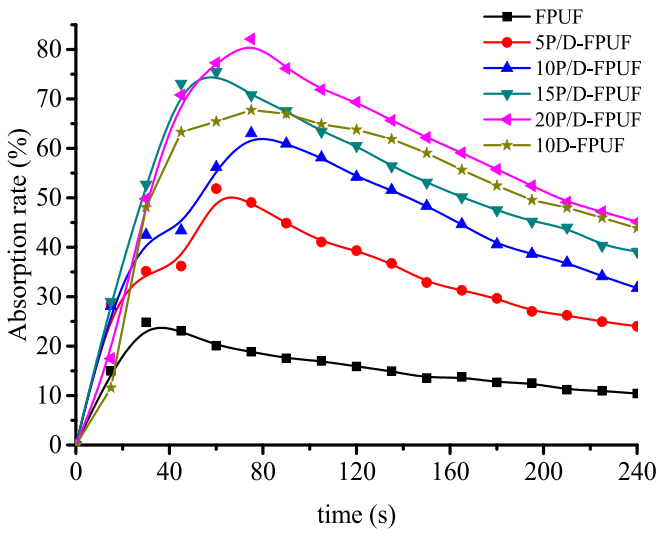

Fig. 10. The absorption rate-time curve of P/D-FPUF with different TPP contents.

retardants. Table 4 presents the maximum smoke density (MSD), the time of MSD (T_{MSD}) and smoke density rating (SDR) for these materials.

As depicted in Fig. 10 and Table 4, the smoke density of FPUF initially increases to a peak value and then it would decrease. Pure FPUF attains a peak smoke density of 25 % within 30 s. The addition of core–shell flame-retardant particles results in a gradual increase in smoke density, but also delays the time to reach maximum smoke density. For instance, with 20 g of core–shell particles added, the peak time extends to 78 s, affording a potentially longer window for evacuation in the initial stages of a fire. This is attributed to the flame retardants capturing free radicals during combustion, curtailing the combustion chain reaction, diminishing combustible gases, and enhancing the foam's flame retardancy, albeit with increased smoke particulate production. Brominated flame retardants are known to generate copious smoke and non-combustible gases when they were burned, decelerating the combustion process (Meng et al., 2023). In addition, the incomplete combustion of DBDPE due to its burning temperature and thermal decomposition products can also increase the generation of smoke (Stubbings and Harrad, 2014; Altarawneh et al., 2019).

A comparison of smoke density data between 10P/D-FPUF and 10D-FPUF samples reveals that the SDR is lower for the core–shell particle-enhanced foam, with 10P/D-FPUF recording an SDR of 45 %. The time to reach maximum smoke density is similar for both samples, which is consistent with the presence of brominated flame retardants in each. However, the method of incorporation is different. In the case of 10P/D-FPUF, core–shell flame retardant particles are grafted onto TDI, causing the polyurethane foam itself to contain flame retardant components. While for 10D-FPUF, DBDPE is added directly without undergoing a chemical reaction with FPUF, resulting in inferior dispersion and compatibility compared to reactive flame retardants. During combustion, DBDPE may release HBr and other volatile substances, which can increase the concentration of smoke (Stubbings and Harrad, 2014; Altarawneh et al., 2019). Consequently, the impact on smoke production is likely to be lower when flame retardants are chemically grafted.

4. Conclusion

This study introduced the synthesis of core–shell flame-retardant particles DBDPE@PMA via emulsion polymerization, with DBDPE as the core and PMA as the shell, which confers both flame retardancy and improved toughness. Scanning electron microscopy verified the encapsulation of DBDPE by a polymer layer, forming a core–shell structure, and confirmed the compatibility of DBDPE@PMA with FPUF. The carboxyl groups on DBDPE@PMA reacted with isocyanate groups, influencing the nucleation reaction and increasing the foam's apparent density. Compared to pure FPUF and 10D-FPUF with only DBDPE added, the FPUF with DBDPE@PMA exhibited an increased apparent density of 1600.9 kg/m^3, an elevated oxygen index value of 33.6 %, and improved horizontal and vertical burning ratings of HB and V-0, respectively. The residual mass after combustion rose to 5.06 %, and the smoke density rating increased to 58 %, with the time to reach maximum smoke density extended to 78 s. DBDPE@PMA demonstrated a smaller impact on FPUF's structure and superior compatibility compared to directly added DBDPE. During combustion, DBDPE's decomposition releases non-combustible gases and water vapor, reducing the heat of combustion. Its gaseous byproducts shield the base material from oxygen and heat, while bromine radicals (Br·) capture hydroxyl radicals (OH·), effectively terminating the combustion chain reaction and suppressing combustion. The development of DBDPE@PMA core–shell flame-retardant particles positively influence the flame retardancy of flexible polyurethane foam.

Table 4
MSD, T_{MSD} and SDR values of P/D-FPUF with different TPP contents.

Sample	MSD (%)	T_{MSD} (s)	SDR (%)
FPUF	25	30	15
5P/D-FPUF	52	60	34
10P/D-FPUF	63	74	45
15P/D-FPUF	75	61	53
20P/D-FPUF	82	78	58
10D-FPUF	68	75	53

CRediT authorship contribution statement

Xuping Ni: Conceptualization, Writing – original draft, Visualization, Investigation, Formal analysis, Methodology, Resources. **Lingjie Wu:** Funding acquisition, Data curation, Writing – review & editing, Validation, Supervision, Project administration.

Declaration of Competing Interest

The authors declare that they have no known competing financial interests or personal relationships that could have appeared to influence the work reported in this paper.

Acknowledgements

The authors gratefully acknowledge the financial support provided by the National Natural Science Foundation of China (52008317).

References

Altarawneh, M., Saeed, A., Al-Harahsheh, M., et al., 2019. Thermal decomposition of brominated flame retardants (BFRs): Products and mechanisms. Prog. Energy Combust. Sci. 70, 212–259. https://doi.org/10.1016/j.pecs.2018.10.004.

Chan, Y.Y., Ma, C., Zhou, F., et al., 2021. Flame retardant flexible polyurethane foams based on phosphorous soybean-oil polyol and expandable graphite. Polym. Degradation. Stab. 191, 109656 https://doi.org/10.1016/j.polymdegradstab.2021.109656.

Chan, Y.Y., Ma, C., Zhou, F., et al., 2022. A liquid phosphorous flame retardant combined with expandable graphite or melamine in flexible polyurethane foam. Polym. Advan. Technol. 33 (1), 326–339. https://doi.org/10.1002/pat.5519.

Eceiza, I., Aguirresarobe, R., Barrio, A., et al., 2023. Ammonium polyphosphate-melamine synergies in thermal degradation and smoke toxicity of flexible polyurethane foams. Thermochim. Acta. 726, 179554 https://doi.org/10.1016/j.tca.2023.179554.

Gao, Z., Yuan, B., Qi, C., et al., 2024. Multi-stage releasing water: The unique decomposition property makes attapulgite function as an unexpected clay mineral-based gas source in intumescent flame retardant. Composites: Part. a. 178, 108014 https://doi.org/10.1016/j.compositesa.2024.108014.

Guo, W.W., Nie, S.B., Kalali, E.N., et al., 2019. Construction of SiO2@UiO-66 core shell microarchitectures through covalent linkage as flame retardant and smoke suppressant for epoxy resins. Compos. Part. B-Eng. 176, 107261 https://doi.org/10.1016/j.compositesb.2019.107261.

Han, S.J., Li, J.P., Ding, Q.Y., et al., 2023. Effects of processing conditions on the properties of monoammonium phosphate microcapsules with melamine-formaldehyde resin shell. Polymers-Basel. 15 (14), 2991. https://doi.org/10.3390/polym15142991.

Karteri, I., Ozyesildag, M., 2021. Structural, thermal, optical, mechanical and morphological properties of ABS/RGO with DBDPE nanocomposites. J. Polym. Mater. 38, 167–177. https://doi.org/10.32381/jpm.2021.38.1-2.13.

Kim, Y., Kim, Y.N., Kim, S.K., et al., 2023. Study on flame retardancy and adhesive properties of hybrid flame retardant composite filler-based polyurethane. Polym-Korea. 47 (4), 513–518. https://doi.org/10.7317/pk.2023.47.4.513.

Lee, J., Park, J.H., Shim, S.B., et al., 2022. Mechanical properties of polypropylene-based flame retardant composites by surface modification of flame retardants. Polymers-Basel. 14 (17), 3524. https://doi.org/10.3390/polym14173524.

Li, Y.M., Hu, W.J., Hu, S.L., et al., 2023b. Fabrication of organic P-N aerogel towards simultaneously super thermal insulation, enhanced compressive strength, flame retardancy and smoke suppression for the rigid polyurethane foam. Chem. Eng. J. 474, 145803 https://doi.org/10.1016/j.cej.2023.145803.

Li, P., Jiang, X.C., Song, W.M., et al., 2023a. An intumescent flame-retardant system based on carboxymethyl cellulose for flexible polyurethane foams with outstanding flame retardancy, antibacterial properties, and mechanical properties. Int. J. Biol. Macromol. 240, 124387 https://doi.org/10.1016/j.ijbiomac.2023.124387.

Li, P., Liu, H., Xu, Y.-J., et al., 2024. Flame-retardant and antibacterial flexible polyurethane foams with high resilience based on a P/N/Si-containing system. J. Mater. Sci. Technol. 182, 141–151. https://doi.org/10.1016/j.jmst.2023.09.030.

Li, C., Wang, D., Liu, C.C., 2008. Preparation and characterization of polymer core shell latex particles. J. Disper. Sci. Technol. 29 (3), 347–350. https://doi.org/10.1080/01932690701716051.

Liu, Y., Li, C., Li, C.X., et al., 2023. Porous, robust, thermally stable, and flame retardant nanocellulose/polyimide separators for safe lithium-ion batteries. J. Mater. 11, 23360–23369. https://doi.org/10.1039/d3ta05148j.

Liu, C., Shi, Y.Q., Feng, Y.Z., et al., 2022. Design of core-multi shell flame retardant towards fire safe thermoplastic polyurethane composites with low toxic fumes generation. Compos. Commun. 35, 101339 https://doi.org/10.1016/j.coco.2022.101339.

Liu, W.J., Tian, K., Jiang, H., et al., 2016. Lab-scale thermal analysis of electronic waste plastics. J. Hazard. Mater. 310, 217–225. https://doi.org/10.1016/j.jhazmat.2016.02.044.

Lu, J.Y., Tu, H.Y., Gu, G.X., 2023. Synthesis of brominated flame retardants with different brominated structures and study on flame retardancy of polystyrene resin. Reactive Funct. Polymers 193, 105769. https://doi.org/10.1016/j.reactfunctpolym.2023.105769.

Meng, D., Gu, W.W., Zhu, G.Y., et al., 2023. Interfacial architecting of long-acting hyperbranched flame retardant with high efficiency towards smoke-suppressed flexible polyurethane foam. Compos. Part. B-Eng. 262, 110816 https://doi.org/10.1016/j.compositesb.2023.110816.

Nabipour, H., Wang, X., Song, L., et al., 2020. Laponite-based inorganic-organic hybrid coating to reduce fire risk of flexible polyurethane foams. Appl. Clay. Sci. 189, 105525 https://doi.org/10.1016/j.clay.2020.105525.

Ni, J.X., Chen, L.J., Zhao, K.M., et al., 2011. Preparation of gel-silica/ammonium polyphosphate core-shell flame retardant and properties of polyurethane composites. Polym. Advan. Technol. 22 (12), 1824–1831. https://doi.org/10.1002/pat.1679.

Ni, X.P., Wu, L.J., 2023. Preparation and Performance Study of a Novel Flame Retardant Polyurethane Phase Change Materials. J. Polym. Environ. https://doi.org/10.1007/s10924-023-03047-x.

Qin, S.Q., Yang, Z.Y., Zhang, S., et al., 2021. Comparison of flame-retardancy property and mechanism between a phosphate ester and a phosphoramine flame-retardants. J. Wuhan. Univ. Technol. 36 (1), 148–156. https://doi.org/10.1007/s11595-021-2388-8.

Rao, W.H., Xu, H.X., Xu, Y.J., et al., 2018a. Persistently flame-retardant flexible polyurethane foams by a novel phosphorus-containing polyol. Chem. Eng. J. 343, 198–206. https://doi.org/10.1016/j.cej.2018.03.013.

Rao, W.H., Zhu, Z.M., Wang, S.X., et al., 2018b. A reactive phosphorus-containing polyol incorporated into flexible polyurethane foam: Self-extinguishing behavior and mechanism. Polym. Degradation. Stab. 153, 192–200. https://doi.org/10.1016/j.polymdegradstab.2018.04.029.

Shi, C.L., Wan, M., Duan, J.H., et al., 2024. Core-shell flame retardants based on Chitosan@MMT coated ammonia polyphosphate for enhancing flame retardancy of polyurethane. Compos. Part. a-Appl. 176, 107831 https://doi.org/10.1016/j.compositesa.2023.107831.

Stubbings, W.A., Harrad, S., 2014. Extent and mechanisms of brominated flame retardant emissions from waste soft furnishings and fabrics: A critical review. Environ. Int. 71, 164–175. https://doi.org/10.1016/j.envint.2014.06.007.

Wang, X.S., Li, L., Tong, Y.J., et al., 2021. Synthesis of core/shell structured zinc borate/silica and its surface charring for enhanced flame retardant properties. Polym. Degradation. Stab. 183, 109432 https://doi.org/10.1016/j.polymdegradstab.2020.109432.

Wang, H.K., Liu, Q., Li, H., et al., 2023. Flame-retardant and smoke-suppressant flexible polyurethane foams based on phosphorus-containing polyester diols and expandable graphite. Polymers-Basel. 15 (5), 1284. https://doi.org/10.3390/polym15051284.

Wang, Y.T., Wang, F., Dong, Q.X., et al., 2017. Core-shell expandable graphite @ aluminum hydroxide as a flame-retardant for rigid polyurethane foams. Polym. Degradation. Stab. 146, 267–276. https://doi.org/10.1016/j.polymdegradstab.2017.10.017.

Xia, L., Lv, Y., Miao, Z.X., et al., 2022. A flame retardant fabric nanocoating based on nanocarbon black particles@polymer composite and its fire-alarm application. Chem. Eng. J. 433, 133501 https://doi.org/10.1016/j.cej.2021.133501.

Ye, L., Meng, X.Y., Liu, X.M., et al., 2009. Flame-retardant and mechanical properties of high-density rigid polyurethane foams filled with decabrominated dipheny ethane and expandable graphite. J. Appl. Polym. 111, 2372–2380. https://doi.org/10.1002/app.29242.

Zhang, S.H., Chu, F.K., Xu, Z.M., et al., 2022. The improvement of fire safety performance of flexible polyurethane foam by Highly-efficient P-N-S elemental hybrid synergistic flame retardant. J. Colloid. Interface. Sci. 606, 768–783. https://doi.org/10.1016/j.jcis.2021.08.069.

Zhang, X.G., Ge, L.L., Zhang, W.Q., et al., 2011. Expandable graphite-methyl methacrylate-acrylic acid copolymer composite particles as a flame retardant of rigid polyurethane foam. J. Appl. Polym. Sci. 122 (2), 932–941. https://doi.org/10.1002/app.34198.

Zhou, F., Zhang, T., Zou, B., et al., 2020. Synthesis of a novel liquid phosphorus-containing flame retardant for flexible polyurethane foam: Combustion behaviors and thermal properties. Polym. Degradation. Stab. 171, 109029 https://doi.org/10.1016/j.polymdegradstab.2019.109029.

Zhu, M.-H., Ma, Z.-W., Liu, L., et al., 2022. Recent advances in fire-retardant rigid polyurethane foam. J. Mater. Sci. Technol. 112, 315–328. https://doi.org/10.1016/j.jmst.2021.09.062.